

CONFOCAL WHITE LIGHT MICROSCOPY

H.-J. Jordan, R. Brodmann, J. Valentin, M. Grigat

NanoFocus Messtechnik GmbH, Bismarckstrasse 120, 47057 Duisburg, Germany, e-mail: info@nanofocus.de

SUMMARY

Non-contact optical techniques for 3D surface data acquisition like short coherence (white light) interferometry, optical profilers or fringe projection are well established for applications with low surface complexity, where the average surface roughness amplitude is small and neglectable compared to the form amplitudes or where the aspect ratios of amplitudes and spacings are small. In general, those optical techniques do not have a good accuracy in reproducing the roughness part of surface data. We present an improved non-contact optical technique, a new confocal white light microscope, which allows a fast access to quantitative 3D topographical acquisition. The results of this new instrument are comparable to those of stylus instrument measurements, even on very complex surfaces.

Keywords: Confocal 3D microscopy, 3D surface analysis, Optical metrology, Optical topometry, Optical profilometry

1 INTRODUCTION

Confocal microscopy, as first described by M. Minski in 1957 (originally named “double focusing microscopy”) [1, 2] becomes a more and more powerful tool for 3D characterisation of complex surfaces.

In reflection mode confocal microscopy, light emitted from a point light source is imaged into the object focal plane of a microscope objective (the first focussing). A in focus specimen location results in a maximum flux of the reflected light through a detector pinhole (the second focussing), whereas light from defocused object regions is partly suppressed. Thus, the detector signal as limited by the pinhole size is reduced strongly when defocusing the specimen [3, 4]. This effects the so called depth discrimination, which allows optical sectioning and contrast enhancement by suppression of light scattered from defocused specimen locations. A further advantage of confocal microscopy against classical light microscopy is an increase of the lateral resolution of about 20% [5].

For xy -scanning, the NanoFocus™ μ Surf™ confocal microscope is using a multiple pinhole mask (Nipkow disk) in an intermediate image plane of a microscope as first described by Petran [6]. Combined with CCD image processing, the rotating Nipkow disk affects a real-time xy -scan of the object field. Just an additional z -scan is necessary for 3D acquisition [7, 8].

2 A SHORT THEORY

A comprehensive description of the theory of confocal microscopy is given in [5], some formulas relevant for 3D topometry are as follows [7 - 9]. The depth response $I(z)$ of a confocal system is proportional to a $SINC^2$ function,

$$I(z) = \left(\frac{\sin(kz(1 - \cos\alpha))}{kz(1 - \cos\alpha)} \right)^2 I_0 \quad (1)$$

which is depending on the aperture angle α of the microscope objective, the wavelength of light λ , the wavenumber $k = 2\pi/\lambda$ and the co-ordinate of

defocusing z . Significant for the depth response $I(z)$ is the Full Width at Half Maximum, which is

$$FWHM = 2z_{1/2} \approx \frac{0,443\lambda}{1 - \cos\alpha} \quad (2)$$

The half angle of the numerical aperture NA determines the maximum surface slope

$$\alpha_{\max}^{spec} = 0.5 \sin^{-1} NA \quad (3)$$

for specular reflection at a microscopic smooth surface element of the specimen. The wavelength together with the numerical aperture determine the full width at half maximum $FWHM$ of the depth response $I(z)$ of the detectors intensity.

Engineering surfaces often have micro-roughness within the probe spot size, therefore diffuse reflection increases the maximum surface slope which can be measured ($\alpha^{diff} \geq \alpha_{\max}^{spec}$) and α_{\max}^{spec} according to equation 3 indicates a lower limit of the surface slope.

3 THE NANOFOCUS™ μ SURF™ 3D CONFOCAL MICROSCOPE

The measurement station (figure 1) consists of a compact confocal module, which includes all the optics.



Figure 1: The μ Surf™ measurement station

An external Xenon lamp is connected to the confocal module via a light guide. The confocal module is fixed on the precise stepper motor driven linear axis which is mounted on a solid bridge stand. For a non-contact measurement of surface topography the sample is positioned using a xy precision slide and the confocal module is moved stepwise in z -direction (Piezo with up to $350\mu\text{m}$ travel and 10nm resolution or precise stepper motor driven linear axis with 100mm travel and 100nm resolution). The measurement station is controlled by software running under MicrosoftTM WindowsTM (98 / NT4, 2000). The surface topographic data can be visualised and analysed in various ways.

The Nipkow disk consists of an array of pinholes arranged in a spiral shape. The rotating disk is illuminated by a plane wave and acts as a scanning multiple point light source, which is imaged into the object focal plane of the microscope objective. After the reflection of light, each illuminating Nipkow pinhole acts as his own detector pinhole. The depth discriminated xy information $I(x,y,z)$ is imaged onto a CCD camera. Thus, during one rotation of the disk, a xy -section of the specimen is acquired in video real-time. Image processing and height evaluation is done using a 512×512 pixel frame-grabber. By an additional z -scan of the specimen, a stack z_1 to z_n ($n < 3000$) of depth discriminated CCD camera-frames is acquired, from which a 3D topography can be constructed with an resolution of about 1% of the FWHM.

In figure 2, a measured depth response $I(x_i, y_j, z)$ and the mode of evaluation of the height coordinate $h(x_i, y_j)$ for example as the centre of $I(x_i, y_j, z)$ is presented.

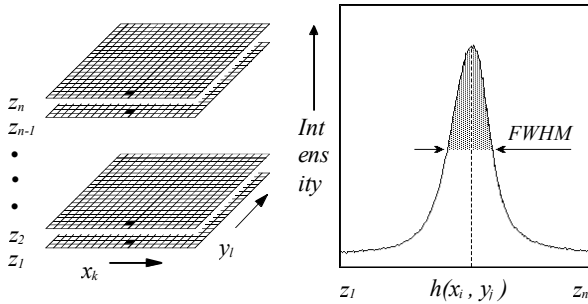


Figure 2: Calculation of the height $h(x_i, y_j)$ as the centre of the depth response $I(x_i, y_j, z)$ for each pixel of the stack z_1 to z_n (topography evaluation).

A well formed depth response is decisive for accurate confocal 3D topometry. Technical data of the $\mu\text{Surf}^{\text{TM}}$ are summarised in Table 1.

The accuracy of the $\mu\text{Surf}^{\text{TM}}$ measurement principle have been approved in all 3 co-ordinates using several standards like the PTB depth setting or the PTB roughness standards [7, 8]. In former comparisons to tactile instruments a very good agreement not only in the profile records but also in roughness parameters was obtained [7, 8].

4 INCREASING THE MICROSCOPES MEASUREMENT FIELD SIZE USING STITCHING

Based on the high accuracy of the $\mu\text{Surf}^{\text{TM}}$ topographic data, a very powerful and effective stitching has been developed in order to overcome the limitation of the single measurement field size [9]. It should be noticed that all presentations within this paper are showing raw data of the $\mu\text{Surf}^{\text{TM}}$ system. No artefacts or spikes have been filtered out in any plot.

For stitching, a set of single measurements with an field overlap between neighboured measurements of about 10% of the single measurement field size were acquired and combined using a correlation algorithm, which works in all 3 axis.

Using the $\mu\text{Surf}^{\text{TM}}$ stitching, the measurement field size can be increased without loss of resolution. Thus, stitching allows one to obtain measurement fields with high spatial and vertical resolution, which are big enough for example for roughness analysis according to the DIN requirements.

5 FRICTION AND WEAR ANALYSIS

Stitching has been used for comparison, visualisation and analysis of a friction test on an EBA steel sheet, according to the requirements of SEP 1940 [10]. Using the $20\times$ microscope objective from table 1 and performing a 25×1 stitching, the required measurement length of 17.5mm was achieved not only for one line profile but for a topography containing about 500 parallel profiles. Such stitching measurements have been carried out before and after the friction test. Figure 3 shows a zoom of the resulting topography ($600\mu\text{m} \times 600\mu\text{m}$) before the friction test and figure 4 the counterpart after the friction test.

Microscope objective	10 \times	20 \times	50 \times	100 \times
Basic field [$\mu\text{m} \times \mu\text{m}$]	1600 \times 1510	800 \times 755	320 \times 302	160 \times 151
Working distance [mm]	10,1	3,1 / 12,0*	0,66 / 10,6*	0,31 / 3,4*
Numerical aperture	0,30	0,46 / 0,40*	0,80 / 0,50*	0,95 / 0,80*
Max. slope for specular reflection [deg.]	8,7	13,7 / 11,7*	26,6 / 15,0*	35,9 / 26,6*
Vertical resolution	50	<30 / <20**	<20 / <10**	<20 / <5**

Table 1: Technical data of the $\mu\text{Surf}^{\text{TM}}$.

* Long working distance

** Piezo for high resolution

Both figures show the 3D topography in photorealistic shading in which the image for the 3D map is superimposed by shadowing effects, caused from a programmable light source. This results in a gradient

enhancement, visualising very fine surface details. The wear effect can clearly be seen from the typical difference in the surface topography visualisations between figure 3 and figure 4.

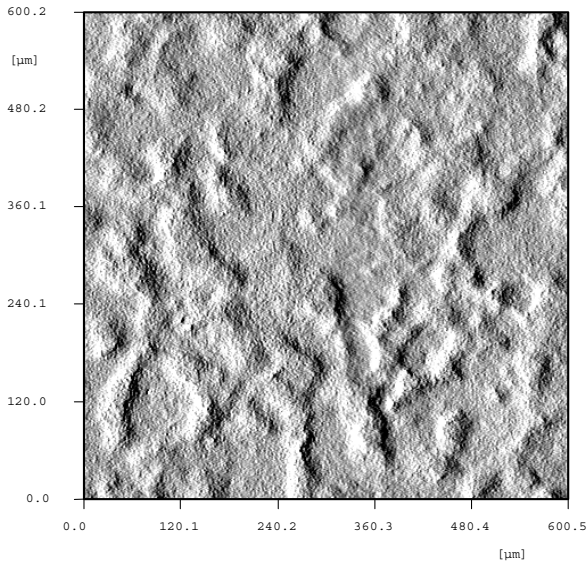


Figure 3: 3D topography of EBA sheet before friction test

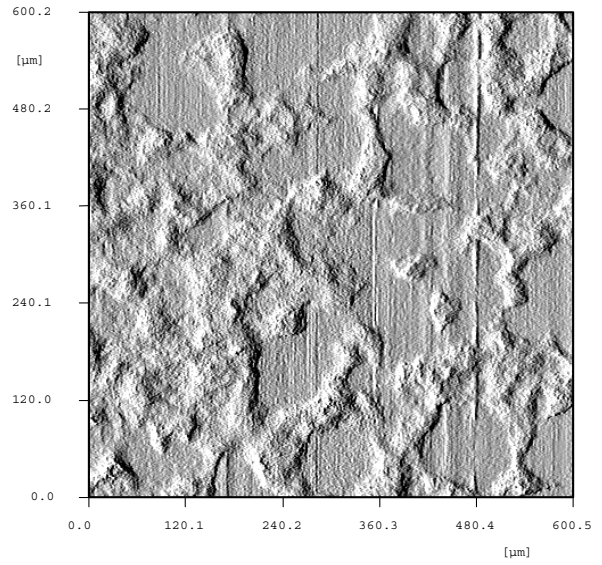


Figure 4: 3D topography of EBA sheet after friction test

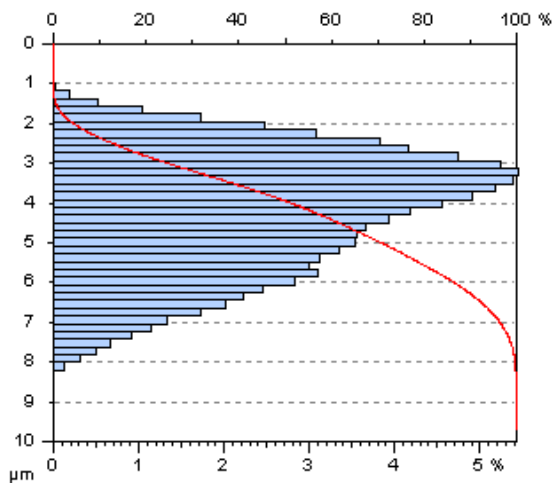


Figure 5: Abbot-Firestone curve of the EBA sheet before the friction test

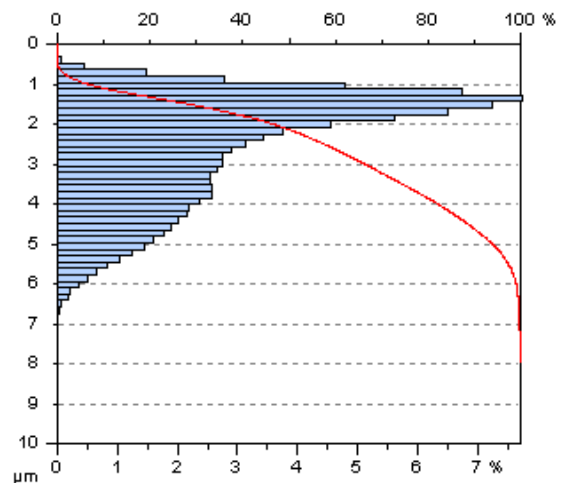


Figure 6: Abbot-Firestone curve of the EBA sheet after the friction test

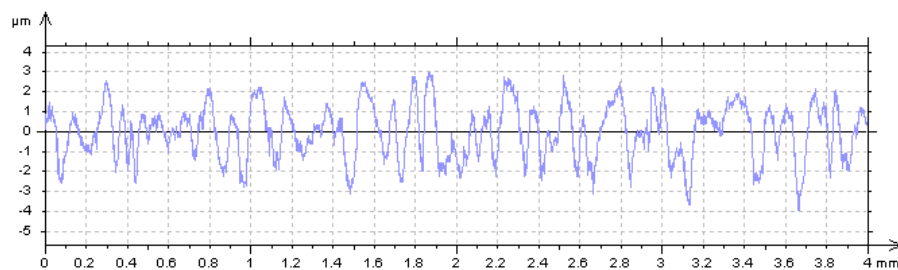


Figure 7: A profile of 4mm length of the EBA sheet before friction test.

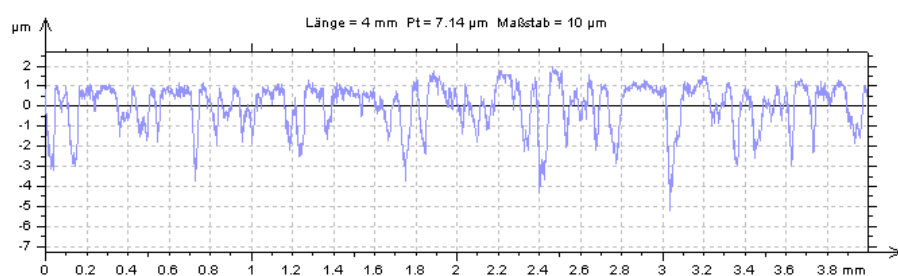


Figure 8: A profile of 4mm length of the EBA sheet after friction test.

It is evident, that wear also has some influence to roughness profiles and parameters, as some of the surface hills have been removed during the friction test. Figure 5 shows the profile height distribution and the Abbott-Firestone curve, figure 7 a typical roughness profile of the EBA sheet before the test, figure 6 and 8 show their counterparts after the test. The wear can clearly be seen both from the sharper upper edge of the profile height distribution (figure 6) as well as the flatter upper envelope of the profile (figure 8). A comparison by numbers is given in table 2.

	EBA, before test	EBA, after test
Mean rough. Ra	1.15 μm	1.05 μm
Skewness R_{SK}	-0.46	-0.79
Kurtosis R_{KU}	2.7	3.1

Table 2: Roughness parameters of the EBA sheet

A further comparison of the topographies in 3D isometric projection is given in figure 9 and figure 10.

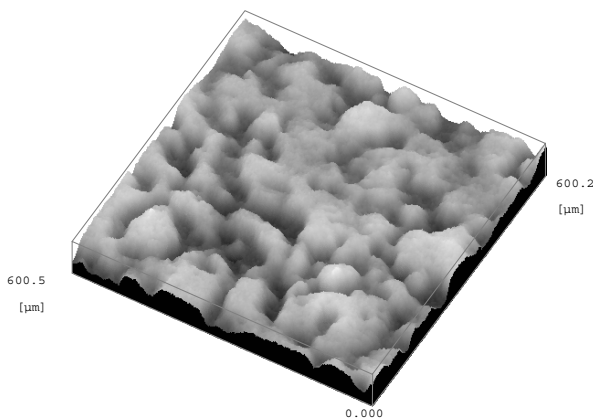


Figure 9: 3D projection of EBA sheet topography, before friction test

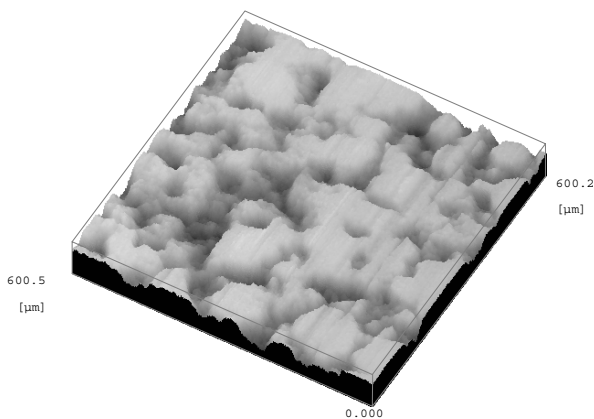


Figure 10: 3D projection of EBA sheet topography, after friction test

6 CONCLUSIONS

The NanoFocus™ $\mu\text{Surf}^{\text{TM}}$ is a powerful instrument for fast and highly accurate non-contact 3D surface topography measurements, even on complex surfaces. Due to the high raw data accuracy, the images in photorealistic shading are – within a comparable resolution in x , y and z - as meaningful as Scanning Electron Microscope images. The results obtained - raw data topographies as well as surface statistics - compare very well to tactile standard techniques. Using the stitching tool large object fields become possible, even for rough and complex engineering surfaces. Thus, the $\mu\text{Surf}^{\text{TM}}$ is an powerful alternative to tactile techniques.

The images in figures 3,4,9 and 10 have been produced using the μsurf Software from NanoFocus. The images in figures 5 - 8 have been produced using the MountainsMap™ software from Digital Surf™.

7 REFERENCES

- [1] Minsky M.: Microscopy Apparatus, U.S. Patent 3013467 (19 Dec. 1961, filed 7 November 1957)
- [2] Minsky M.: Memoir on Inventing the Confocal Scanning Microscope, Scanning 10(4) (1988), 128-138
- [3] Hamilton D. K., Wilson T., and Sheppard C. J. R.: Experimental observation of the depth-discrimination properties of scanning microscopes, Opt. Lett. 6 No 12 (1981), 625
- [4] Wilson T.: Depth response of scanning microscopes, Optik 81 No 3 (1989), 113
- [5] Wilson T.: Confocal Microscopy, Academic Press, 1990
- [6] Petran M., Hadravsky M., Egger M. D. and Galambos R.: Tandem-Scanning Reflected-Light Microscope, J. Opt. Soc. Am. 58(5) (1968), 661
- [7] Jordan H.-J., Wegner M., and Tiziani H.: Optical topometry for roughness measurement and form analysis of engineering surfaces using confocal microscopy, 9th International Precision Engineering Seminar / 4th International Conference on Ultraprecision in Manufacturing Engineering, May 1997, Braunschweig / Germany, ISBN 3-9801433-9-2
- [8] Jordan H.-J., Wegner M., and Tiziani H.: Highly accurate non-contact characterisation of engineering surfaces using confocal microscopy, Meas. Sci. Technol. 9 (1998), 1142-1151
- [9] Jordan, H.-J., Brodmann, R.: Highly accurate surface measurements by means of white light confocal microscopy, X. International Colloquium on Surfaces, January 31st – February 2nd, 2000, Chemnitz / Germany, ISBN 3-8265-6999-7
- [10] Stahl-Eisen-Prüfblatt SEP 1940: Measurement of roughness average Ra and peak count R_pc on cold rolled steel sheet with stochastic surface textures, 2nd edition (1997), Verlag Stahleisen GmbH, Postbox 105164, 40042 Duesseldorf / Germany